ORGANIC LETTERS

2009
Vol. 11, No. 21
4942−4945

Synthesis and Electronic Properties of Isotruxene-Derived Star-Shaped Ladder-Type Oligophenylenes: Bandgap Tuning with Two-Dimensional Conjugation

Jye-Shane Yang,* Hsin-Hau Huang, Yi-Hung Liu, and Shie-Ming Peng

Department of Chemistry, National Taiwan University, Taipei, Taiwan 10617

jsyang@ntu.edu.tw

Received September 10, 2009

ABSTRACT

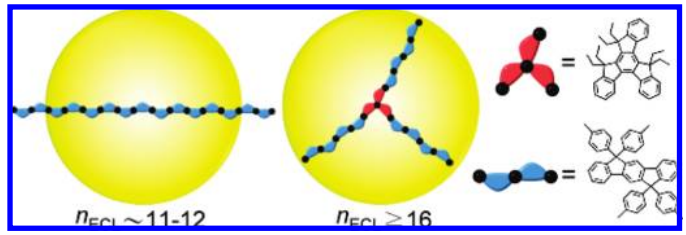

The synthesis of star-shaped ladder-type oligophenylenes S*n* (*n* = 4, 7, 10, 13, and 16), where *n* is the number of π-conjugated phenylene rings, is reported. The two-dimensional conjugation interactions in S*n* result in a lower bandgap for S16 than the currently known ladder-type poly(*p*-phenylene)s (LPPPs).

Phenylene-based oligomers and polymers are potential electronic materials for use in light-emitting diodes and polymer lasers.[1−4] A variety of phenylene scaffolds, differing in dimensions and rigidity of the π-backbones, have been explored[1−13] to construct the structure−property relationships. Nevertheless, examples of star-shaped ladder-type (SL) systems are rare.[9] A SL phenylene system demands a core unit such as truxene (**1**) and isotruxene (**2**). We have recently shown that the para-ortho-branched isotruxene core allows strong electronic couplings among the branched arms.[12,13] We report herein the synthesis and characterization of a series of isotruxene-based SL oligophenylenes **S*n***, where *n* is the

(1) (a) Grimsdale, A. C.; Müllen, K. *Adv. Polym. Sci*. **2006**, *199*, 1–82. (b) Grimsdale, A. C.; Müllen, K. *Adv. Polym. Sci*. **2008**, *212*, 1–48.
(2) (a) Grimme, J.; Scherf, U. *Macromol. Chem. Phys*. **1996**, *197*, 2297–2304. (b) Grimme, J.; Kreyenschmidt, M.; Uckert, F.; Müllen, K.; Scherf, U. *Adv. Mater*. **1995**, *7*, 292–295.
(3) Gierschner, J.; Cornil, J.; Egelhaaf, H.-J. *Adv. Mater*. **2007**, *19*, 173–191.
(4) Banerjee, M.; Shukla, R.; Rathore, R. *J. Am. Chem. Soc*. **2009**, *131*, 1780–1786.
(5) Schindler, F.; Jacob, J.; Grimsdale, A. C.; Scherf, U.; Müllen, K.; Lupton, J. M.; Feldmann, J. *Angew. Chem., Int. Ed*. **2005**, *44*, 1520–1525.
(6) Wong, K.-T.; Chi, L.-C.; Huang, S.-C.; Liao, Y.-L.; Liu, Y.-H.; Wang, Y. *Org. Lett*. **2006**, *8*, 5029–5032.
(7) Wu, Y.; Zhang, J.; Fei, Z.; Bo, Z. *J. Am. Chem. Soc*. **2008**, *130*, 7192–7193.
(8) Wu, Y.; Zhang, J.; Bo, Z. *Org. Lett*. **2007**, *9*, 4435–4438.
(9) Zhang, W.; Cao, X.-Y.; Zi, H.; Pei, J. *Org. Lett*. **2005**, *7*, 959–962.
(10) (a) Kanibolotsky, A. L.; Berridge, R.; Skabara, P. J.; Perepichka, I. F.; Bradley, D. D. C.; Koeberg, M. *J. Am. Chem. Soc*. **2004**, *126*, 13695–13702. (b) Lai, W.-Y.; Chen, Q.-Q.; He, Q.-Y.; Fan, Q.-L.; Huang, W. *Chem. Commun*. **2006**, 1959–1961. (c) Han, Y.; Fei, Z.; Sun, M.; Bo, Z.; Liang, W.-Z. *Macromol. Rapid Commun*. **2007**, *28*, 1017–1023. (d) Zhang, W.-B.; Jin, W.-H.; Zhou, X.-H.; Pei, J. *Tetrahedron* **2007**, *63*, 2907–2914. (e) Jiang, Y.; Lu, Y.-X.; Cui, Y.-X.; Zhou, Q.-F.; Ma, Y.; Pei, J. *Org. Lett*. **2007**, *9*, 4539–4542.
(11) (a) Sun, Y. M.; Xiao, K.; Liu, Y. Q.; Wang, J. L.; Pei, J.; Yu, G.; Zhu, D. B. *Adv. Funct. Mater*. **2005**, *15*, 818–822. (b) Wang, J.-L.; Luo, J.; Liu, L.-H.; Zhou, Q.-F.; Ma, Y.; Pei, J. *Org. Lett*. **2006**, *8*, 2281–2284. (c) Wang, J.-L.; Yan, J.; Tang, Z.-M.; Xiao, Q.; Ma, Y.; Pei, J. *J. Am. Chem. Soc*. **2008**, *130*, 9952–9962.
(12) Yang, J.-S.; Huang, H.-H.; Ho, J.-H. *J. Phys. Chem. B* **2008**, *112*, 8871–8878.
(13) Yang, J.-S.; Lee, Y.-R.; Yan, J.-L.; Lu, M.-C. *Org. Lett*. **2006**, *8*, 5813–5816.

10.1021/ol9021035 CCC: $40.75
Published on Web 10/05/2009

number of π-conjugated phenylene rings (Figure 1). Our results show explicitly that exciton in **S*n*** can delocalize over the whole π-backbone up to 16 phenylene rings, a size that is beyond the effective conjugation length (ECL) of 11−12 rings defined[3,5] by the rod-shaped ladder-type (RL) counterparts (R*n*).

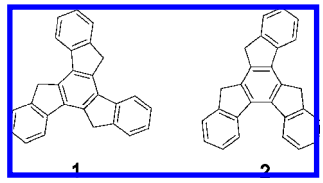

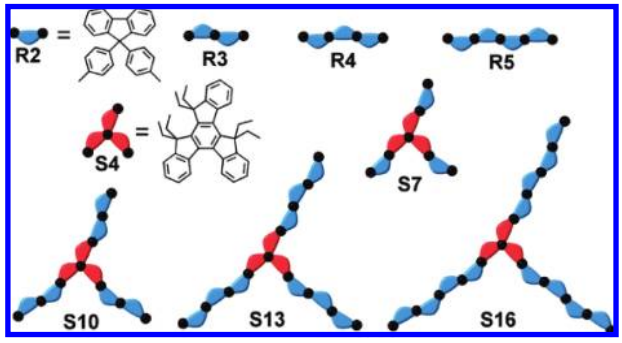

Figure 1. Schematic representation of the structures of oligophenylenes **R*n*** and **S*n***, where the black dots represent the π-conjugated phenylene rings with a number of *n*.

The synthesis of **S*n*** adopts the commonly used strategy for the synthesis of RL systems.[5,6] A typical example by the case of **S7** is shown in Scheme 1, in which the Suzuki−Miyaura reaction between **S4BA** and **A1** elongates the π-backbone and the subsequent nucleophilic carbonyl addition and intramolecular Friedel−Crafts alkylation reactions form the ladder scaffold. The synthesis of building blocks isotruxene **S4** and isotruxene tribromide **S4Br** was recently reported.[13,14] This synthetic protocol also applied to **S10**, **S13**, and **S16** simply by replacing **A1** with the longer arm precursors **A2**, **A3**, and **A4**, respectively. The synthetic details can be found in the Supporting Information.

Figure 2a shows the electronic absorption and fluorescence spectra for **S4**, **S7**, **S10**, **S13**, and **S16** in dichloromethane. Except for the fluorescence spectrum of **S4**, all the spectra display well-defined 0−0 vibronic bands, and they undergo a bathochromic shift with increasing number of phenylene rings. Oligophenylenes **S*n*** retain the features of high fluorescence quantum yield (Φ_{fl}) generally observed for RL systems. The corresponding photophysical data are shown in Table 1. For better comparison, the known RL systems **R2**−**R5**[6] were prepared and investigated under the same experimental conditions. We found that the wavelengths of the 0−0 absorption and fluorescence bands for **R3**−**R5** in CH_2Cl_2 are essentially the same as those for the corresponding spiro-fluorene substituted RL systems **R′3**−**R′5** in CH_2Cl_2 or toluene.[8] This indicates that the larger system **R′8** (λ_{abs} = 433 nm and λ_{fl} = 441 nm) reported in the same paper[8] can also be used for comparison (see Figures 2b and 2c).

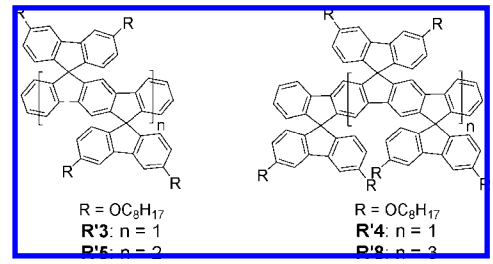

The most important findings of these spectral data are that (a) **S*n*** (n = 4, 7, 10, 13, 16) and **R*n*** (n = 2−5 and 8) fall in the same linear correlation ($r^2 > 0.99$) for the 0−0 band energies of either absorption or fluorescence against the reciprocal of number of π-conjugated phenylene rings (i.e., 1/*n*) and that (b) there is no sign of saturation in the plots even with **S13** and **S16** (Figure 2b and 2c). The former observation suggests that excitation is effectively delocalized over the two-dimensional (2D) π-backbone of **S*n*** in both the ground- and excited-state configurations. To the best of our knowledge, similar behavior has not been reported for the other star-shaped conjugated oligomers.[9−12] We could ascribe the strong electronic couplings among the arms of

Scheme 1. Synthesis of **S7** from **S4** and Structures of **A1**−**A4**

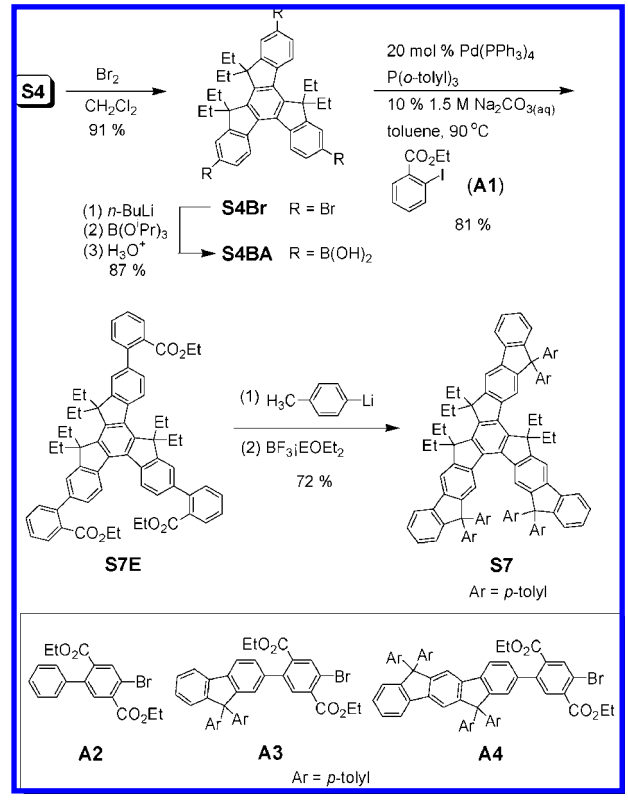

(14) Yang, J.-S.; Huang, H.-H.; Lin, S.-H. *J. Org. Chem.* **2009**, *74*, 3974–3977.

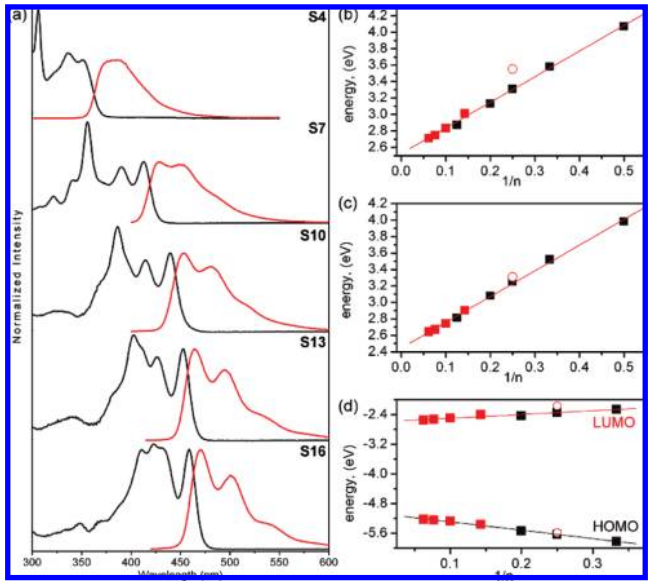

Figure 2. (a) Normalized absorption (black) and fluorescence (red) spectra for **S4**, **S7**, **S10**, **S13**, and **S16**, and linear plots of (b) absorption and (c) fluorescence 0−0 transition energy (eV) and (d) HOMO and LUMO energy levels (eV) versus the reciprocal of number of π-conjugated phenylene rings (1/*n*) for both **S*n*** (red squares) and **R*n*** (black squares). The red open circle specifically denotes **S4** for the purpose of discussion.

S*n* to both the ortho-para-branched isotruxene core and the torsion-constrained π-scaffold. The latter observation further indicates that the ECL of 11−12 phenylene rings defined by RL systems[4,5,15] describes only one dimension of the region allowed for exciton delocalization. We tentatively propose that the maximum chromophore size of effective conjugation interactions covers a cyclic region with a diameter equivalent to the one-dimensional (1D) ECL (Figure 3).[16] As a result of the second dimensional conjugation, **S16** possesses a fluorescence maximum at longer wavelength (470 vs 464 nm)[17] than a recently reported long-chain RL polymer (i.e., a ladder-type poly(*p*-phenylene) (LPPP) of $M_w = 62.0$ kDa).[7]

It is noted that with the same number of phenylene rings for **S4** and **R4** the former deviate from the line toward a higher absorption energy (Figure 2b). This could be attributed to a less planar π-backbone due to a small twist

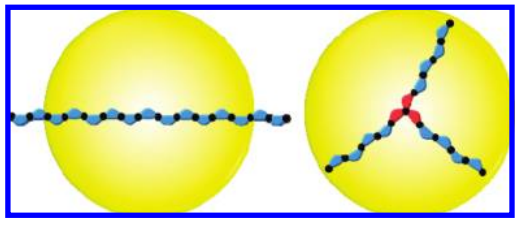

Figure 3. Model proposed for the effective conjugation size (a two-dimensional region covered by the yellow circle) of conjugated polymers illustrated with **R16** and **S16**.

Table 1. Photophysical and Electrochemical Data for **S*n*** and **R*n*** in CH_2Cl_2

compd	λ_{abs}[a] (nm)	logϵ[b]	λ_{fl}[c] (nm)	$\Delta\nu_{st}$[d] (cm^{-1})	Φ_{fl}	τ_{fl} (ns)	E_{ox1}[e] (V)
S4	352	4.19	382[f]	2231	0.55	3.22	0.79
S7	412	4.81	428	907	0.73	1.97	0.57
S10	439	5.03	453	704	0.87	1.38	0.48
S13	452	5.21	464	572	0.87	1.16	0.44
S16	458	5.27	470	557	0.89	1.03	0.43
R2	305	3.85	312	736		4.04	
R3	347	4.63	353	490	0.41	2.01	1.02
R4	375	4.88	382	489	0.72	1.36	0.83
R5	396	5.04	403	439	0.75	1.12	0.75

[a] Maximum of the 0−0 absorption band. [b] Extinction coefficient of the 0−0 absorption band. [c] Maximum of the 0−0 fluorescence band. [d] Stokes shift defined by the difference of λ_{abs} and λ_{fl}. [e] Potentials were recorded vs ferrocene/ferrocenium. [f] Estimated from the blue edge of the fluorescence plateau.

(9.8°) between the two ortho-branched arms, as shown by the X-ray crystal structure (Figure 4a). A smaller deviation for **S4** in the fluorescence plot (Figure 2c) is consistent with the expected structural relaxation (planarization) in the excited state. This steric effect is negligible for **S7** and the larger **S*n*** systems, although the twist is even larger (e.g., 18.6° for **S7**, Figure 4b) due to the tolyl substituents. This reflects a dilution of wave function in the isotruxene core. The increased Stokes shift ($\Delta\nu_{st}$) on going from **R*n*** to **S*n*** and from **S16** to **S4** (Table 1) also reflects the steric and the chain length effects, respectively.

It should also be noted that the absorption spectra of **S*n*** display more bands at shorter wavelengths (e.g., 300−375 nm for **S7**) in addition to the 0−0 and 0−1 absorption bands that mirror the fluorescence spectra. These short-wavelength absorption bands can be attributed to localized excitation of the ortho-branched arm of **S*n***, which contains $(n + 2)/3$ phenylene rings, as those of **S4**, **S7**, **S10**, and **S13** match reasonably well in positions (306, 356, 386, and 402 vs 305, 347, 375, and 396 nm) with the absorption bands of **R2**, **R3**, **R4**, and **R5**, respectively.

Table 1 also shows the first oxidation potentials (E_{ox1}) of **S*n*** ($n = 4$, 7, 10, 13, 16) and **R*n*** ($n = 3$−5) in dichloromethane determined by cyclic and differential pulse voltammetries (Figure S1, Supporting Information). A linear correlation between E_{ox1} and 1/*n* was observed (Figure S2, Supporting Information). Figure 2d shows the corresponding

(15) The exact ECL of ladder-type polyphenylenes (LPPP) is not well defined. It has also been suggested[1] to be 14−15 phenylene rings based on the fluorescence wavelength determined by single molecule spectroscopy. It should also be noted that the ECL of nonladder-type poly(*p*-phenylene)s was suggested to be larger ($n \sim 20$) than that of LPPP.[2]

(16) According to the model of Figure 3, a saturation of transition energy might be reached at **S19** or **S22**. However, attempts to prepare them were unsuccessful, presumably due to poor solubility of the intermediates. New design and synthesis toward larger and soluble 2D ladder-type polyphenylenes are in progress.

(17) Values reported for compounds in chloroform. The maximum of fluorescence 0−0 band for **S16** in chloroform is the same as that in dichloromethane.

plots with the HOMO and LUMO energy levels derived according to eqs 1 and 2:[18]

$$E_{HOMO} = -(4.8 + E_{ox1}) \quad (1)$$

$$E_{LUMO} = E_{HOMO} + E_{0,0} \quad (2)$$

where $E_{0,0}$ is the 0−0 transition energy obtained from the intersection of normalized absorption and fluorescence 0−0 bands. The larger slope for the HOMO (−2.26) vs LUMO (1.01) plot reveals that the chain length effect on optical bandgap is mainly due to perturbations of the HOMO energy levels. For **S7** and the larger **S*n*** systems, more than one oxidation potential was recorded and the number increases as the *n* value increases (Table S2, Supporting Information), which indicates their ability to accomondate more than one polarion (radical cation). This phenomenon has been observed and elucidated for the stepladder analogues of **S*n***.[12]

In summary, we have synthesized a series of para-ortho-branched SL oligophenylenes **S*n***, in which **S16** is thus far the largest monodisperse ladder-type oligophenylene. The observation of effective exciton delocalization over the 2D conjugated backbones of **S*n*** opened up a new venue for tuning the optical bandgap of conjugated oligomers and polymers.

(18) Pommerehne, J.; Vestweber, H.; Guss, W.; Mahrt, R. F.; Bässler, H.; Porsch, M.; Daub, J. *Adv. Mater.* **1995**, *7*, 551–554.

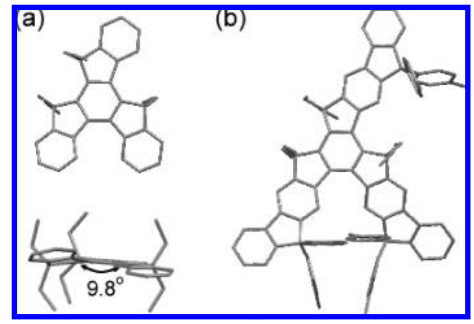

Figure 4. X-ray crystal structures of (a) **S4** (top and side views) and (b) **S7** (top view).

Acknowledgment. We thank the National Science Council of Taiwan, ROC, for financial support.

Supporting Information Available: Experimental methods, synthetic procedures, characterization data, cyclic and differential pulse voltammograms, and the $E_{ox1} - 1/n$ plot for **S*n*** and **R*n*** and CIF for **S4** and **S7**. This material is available free of charge via the Internet at http://pubs.acs.org.

OL9021035